20th International Conference on Structural Mechanics in Reactor Technology (SMiRT 20)
Espoo, Finland, August 9-14, 2009
SMiRT 20-Division 1, Paper 1998

Experimental and Numerical Investigation of Cyclic Thermal Shock at the Paul Scherrer Institute

M. Niffenegger, K.G.F. Janssens & K. Reichlin

Nuclear Energy and Safety Research Department, Paul Scherrer Institute, 5232 Villigen, Switzerland,
e-mail: *Markus.Niffenegger@psi.ch*.

Keywords: Cyclic Thermal Shock, Thermo-Mechanical Fatigue, Turbulent Mixing Phenomena, Plant Life Management

1 ABSTRACT

Specific thermo-hydraulic conditions may lead to cyclic thermal shocks in the piping of the primary circuit of light water reactors. The Civeaux-1 incident occurred more than then years ago, but nevertheless there is still a lack of knowledge concerning the conditions under which a crack network develops and the question when the growth of single cracks results in failure of components.

The Plant Life Management (PLiM) project at the Paul Scherrer Institute (PSI) is dedicated to the analysis of thermo-hydraulic mixing phenomena and to the analysis of crack initiation and growth due to the resulting cyclic thermal shocks on the inner wall of the piping. The project, which includes both experimental investigations and numerical simulations of the complex behavior of fluid and piping material, contributes to a better understanding of the observations made in nuclear power plants.

In the cyclic thermal shock experiments, performed on notched specimens made out of austenitic stainless steels AISI 321, 347 and 316L, cracks of a length up to a few hundred micrometers were initiated at the root of notches with a radius of 0.05 mm and depths of 1 mm and 0.5 mm, by pure thermal load. The finite element calculations have shown the importance and the difficulties of considering cyclic plasticity if softening of austenitic stainless steels takes place. Precise simulations of hundreds of cycles indicated the accumulation of localized ratcheting strains.

The ongoing research activities at PSI in the field of thermo-mechanical fatigue are discussed. In particular, a cyclic thermal shock facility allowing experiments under well defined loading and boundary conditions is described. Finite element calculations considering cyclic plasticity are used to simulate the thermal shock experiments and to compute the stress strain history. The number of cycles needed for crack initiation was evaluated based on the cyclic strain amplitude and the fatigue life curve. It was found that the Smith-Watson-Topper (SWT) correction can be applied to predict the number of cycles to crack formation, if calibration factors are used in the SWT correction. These factors were found in dedicated additional fatigue tests on notched specimens. Furthermore, basic questions regarding the application of such numerical assessment tools are briefly discussed.

2 INTRODUCTION

The goal of the project PLiM at the Paul Scherrer Institute (PSI) is the investigation of fatigue crack initiation and propagation due to cyclic thermal shocks, which may occur in components of the primary circuit of nuclear power plants. The project is dedicated therefore to the experimental and theoretical investigation of thermo-mechanical fatigue (TMF) due to cyclic thermal shocks (CTS). Even though most of the TMF modes are anticipated in the design rules, in special cases unforeseen thermal loads may cause failures in safety relevant components. Therefore appropriate lifetime prediction tools are required.

In nuclear power plants (NPP) the phenomenon of TMF may appear in the low cycle (LCF) or/and in the high cycle (HCF) regime and is usually connected with [NEA/CSNI/R(2005)]:

- Operating transients (LCF, covered by existing rules and codes)
- Stratification due to temperature differences in horizontal tubes (LCF, partially covered by national rules)

- Mixing of cold and hot water flow, e.g. in T-junctions (LCF and HCF, not anticipated at the design stage and therefore not covered by design rules)

In particular CTS, caused by unstable turbulent flow appearing by mixing cold and hot water streams is leading to corresponding temperature fluctuations at the inner wall of the piping, where the induced thermal stresses may end up in a network of micro cracks (elephant skin). The elephant skin, also called crazing, is characteristic for the biaxial stress/strain state due to thermal shocks. Although most micro cracks arrest below a depth of approximately 2 millimeters, under certain circumstances, some of them may grow through the wall as reported in several publications [Faidy (2000), Cipiere et al. (2001, 2002), Hirsberg (2000), Deardorff (2004)]. Such damage was not anticipated at the design stage but observed in some mixing tees. However, in spite of the common agreement concerning the origin of this damage, the exact conditions responsible for macroscopic failures are still unknown and there is still a lack of tools for the reliable prediction of the turbulences, crack initiation and crack growth under operating conditions. In particular the following questions still need to be answered:

- Under which flow conditions do the thermal fluctuations appear? (Thermohydraulic problem)?
- What are the critical locations for crack formation in the primary loop of a LWR?
- What are the temperature differences ΔT and frequencies ω of these fluctuations?
- Which conditions (ω, ΔT, mean temperature T_m, pressure) have to be fulfilled for the initiation and growth of thermally induced cracks?
- How deep do these cracks grow? Under what conditions do they arrest?
- What are the differences between different austenitic stainless steels?
- What is the difference between unilateral (hot-cold) and bilateral (cold-hot-cold) thermal shocks?
- What are the reliable mathematical (deterministic and probabilistic) models for fatigue life prediction?

Answering the above questions and developing computational tools for the prediction of such phenomena are therefore the main goals of the project PLiM which consists of thermal shock experiments, numerical modelling of computational fluid dynamics and structural mechanics by the finite element method as well as material testing and analysis.

Of special interest is the question whether the materials behaviour under bilateral thermal shocks differs from that under unilateral ones, which were widely investigated in the context of emergency cooling transients. In order to investigate these questions, a dedicated thermal shock facility, which allows applying cyclic thermal shocks on notched test specimens, has been built and put into operation by our project partner Siempelkamp Prüf- und Gutachtergesellschaft GmbH in Dresden. Finally a set of austenitic stainless steels specimens (AISI 321, AISI 316L and AISI 347) were tested by two kind of cyclic thermal shocks, namely unilateral and bilateral ones.

Beside the thermal shock experiments and extensive material testing, the project also includes the development of appropriate numerical tools for lifetime prediction [Janssens (2009)]. These numerical tools are advanced Finite Element Methods (FEM) and Computational Fluid Dynamics Methods (CFD), whereas CFD and FEM are coupled by an interface that allows the transfer of the calculated temperature fluctuations from the CFD-code to the FEM-program. This allows the calculation of stress/strains and fracture mechanics parameters for real transient load on relevant geometries.

Since the thermal load is induced by fluctuating turbulent fluid flow, its calculation is of utmost importance. Therefore, different Computational Fluid Dynamics (CFD) methods were evaluated. Beside Large Eddy Simulation (LES), detached Eddy Simulation (DES) and Scale-Adaptive Simulations (SAS) show to be appropriate methods, which provide accurate results within an acceptable computing time. Reasonable dominant frequencies of fluid fluctuations were found by the simulation of a T-junction experiment. The modelling activities are accompanied by thermo-hydraulic experiments which are compared with the CFD calculations. However, this part of the project is not reported in this contribution.

Advanced assessment of thermal fatigue also includes crack growth calculation. However, state-of-the-art FEM-codes have the disadvantage that the crack path has to be defined (along element boundaries), even when it is not known a priori. In order to overcome these shortcomings, special effort is put to the implemen-

tation of Extended Finite Elements (XFEM) into our FEM-code. Such enriched elements allow crack growth calculations without the time consuming remeshing and without predefining the crack path. Since their element description is enriched by singular and unsteady functions, the crack can be inside the finite elements and the stress singularity at the crack tip is better approximated than in conventional finite elements.

A remaining question is the role of ratcheting as found in the experiments and FE-calculations. Especially the influence of, and the difference between compressive and tensile ratcheting, as found in the calculations, on crack initiation and growth is not yet quantified. A PhD thesis is dedicated to this topic in order to investigate cyclic plasticity and to improve the understanding and prediction of cyclic hardening/softening and ratcheting phenomena.

Cyclic plasticity at elevated temperatures will also be investigated in a precompetitive research collaboration with our partners ETHZ, EMPA, ABB Turbo Systems and Alstom, in the framework of the Competence Centre of Materials Science and Technology (CCMX) of Switzerland.

In the following sections the focus is set on the thermal shock experiments and their modelling, some results of the fatigue testing are also included.

3 EXPERIMENTAL SETUP

3.1 Thermal Shock Facility

A set of thermal shock experiments has been performed to investigate fatigue crack initiation and crack growth driven by uni- and bilateral cyclic thermal shocks, which may occur due to fluctuations of hot and cold pressurized water in piping. The CTS experiments are carried out by our project partner Siempelkamp Prüf- und Gutachtergesellschaft GmbH, Dresden.

In the CTS experiments the geometry and governing conditions of the real tubes were mapped into a well defined experimental setup. Therefore, hot and cold oil (UCOTHERM FG-8® from FRAGOL GmbH) with temperatures ranging from 50°C to 250°C was used to apply CTS on the inner wall of a notched disc. The reason for substituting water with oil is that the latter needs not be pressurized at these temperatures, which substantially reduces the complexity of the experimental equipment.

Fig. 1 shows the functional schematic of the thermal shock facility consisting of three loops. One loop exists of a hot and cold storage tank (200 l), a pump, and a heater. The second loop exists of a cold storage tank (200 l), a cooler (type AERMEC), a heat exchanger and a pump. The third loop is separated from the hot and cold ones by control valves, which control the input of cold or hot oil from the two loops mentioned above into the third loop. The test specimens are placed in parallel the third loop. A control unit (type JUMO IMAGO 500) allows the periodic flow of hot and cold oil through the samples.

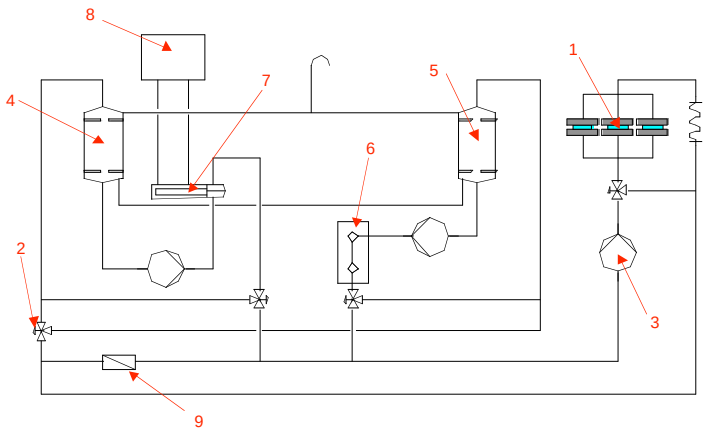

1 test specimens
2 control valve
3 pump
4 cold oil tank
5 hot oil tank
6 electrical heating
7 heat exchanger
8 cooler
9 non-return valve

Fig. 1: Functional schematic of the thermal shock facility.

As shown in Fig. 2, the test specimens are fixed between two flanges in a vertical part of the oil loop, whereas the oil is flowing upwards. In order to increase the flow velocity of the oil and therefore the heat transfer at the inner wall of the specimen, an extrusion body is placed in the flow. The oil velocity at sample location is about 5.36 m/s, resulting in a heat-transfer coefficient of about 7700 W/m^{2}K [Lässig (2007)]. Since the samples are insulated by Kautasit-Aramid sealing, the heat conduction in axial direction is negligi-

ble. The outer wall of the sample is exposed to the ambient temperature of about 40 °C, the heat transfer at this surface is about 40 W/m^{2}K. Four springs ensure the free thermal dilatation of the discs and leak-tightness. Therefore, no relevant axial force is imposed to the discs and the circumferential stress is induced by the radial temperature gradient only.

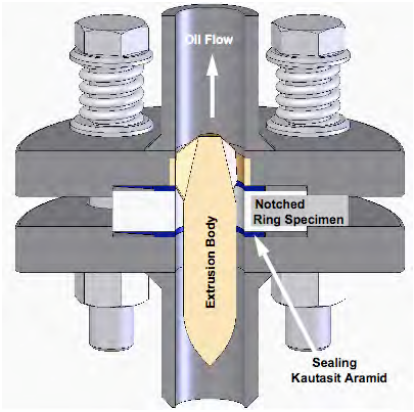

Fig. 2: Schematic showing the mounting of the ring specimen in the sample holder. the oil is flowing through the centre of the ring specimens.

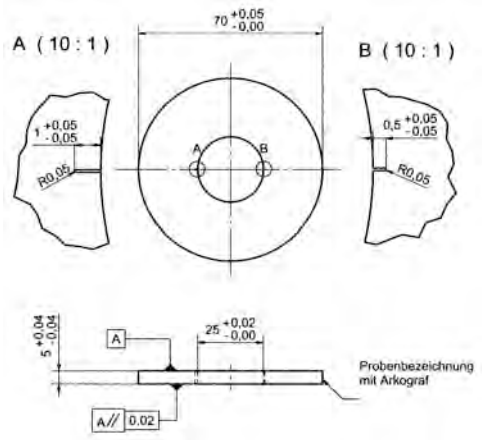

Fig. 3: Notched specimen for CTS tests. The thermal boundary conditions are: T_{oil} = f(t) and h = f(t) at d = 25 mm, h = 40 W/m^{2}K at D = 70 mm.

3.2 Test Specimen

The CTS specimens are made from a low-carbon (AISI 316L, DIN 1.4404) and a Ti- (AISI 321, DIN 1.4541) and Ni-stabilized (AISI 347, DIN 1.4550) austenitic stainless steels. It is worth mentioning that the test specimens are manufactured from bar material and do not fulfil the requirements of nuclear installations. The geometry of the CTS specimen is given in Fig. 3 and the thermal boundary conditions are mentioned in the figure caption. This simple geometry with well defined boundary conditions was selected to allow comparing the concerning results with the numerical simulation. All the surfaces of the specimens have a surface quality of N6. The two wire-cut notches at the inner surface have a width of 0.1 mm and a depth of 1 mm and 0.5 mm, respectively. Since the notches are leading to a stress concentration, they define the location of the deliberate crack initiation. Although the notches do not really reflect the normal condition in a piping, they simplify the experimental observations and its analysis.

3.3 Thermal Loading History

Thermal loading of the specimen's inner surface was chosen to allow crack initiation within a reasonable time limit. Because the frequency of the cyclic thermo-shock is limited by the experimental facility and is far away from that expected in the turbulent flow conditions of mixing tees which are in the order of 1 to 10 Hz, a larger temperature difference was applied to reduce the experimental time. This applied load corresponds more likely to the conditions in emergency cooling transient than to the cyclic thermal shocks in mixing tees. The chosen CTS frequency was chosen in such a way that cooling (heating) of the whole specimen down (up) to the oil temperature could take place after the initial shock. As a consequence, the induced stresses will move from the inner to the outer radius along with the temperature profile. This in principle allows a crack, once initiated at the inner surface, to grow through the wall. This is in contrast to the high cycle behaviour in which the temperature fluctuations and therefore the induced stress are limited to the inner near surface region because the penetration depth is a function of the frequency. In fact, the observations made in reactor components also confirm that most of the detected cracks did not grow deeper than 2 mm.

As shown in Fig. 4, two kinds of CTS were applied at the inner surface of the specimen, namely uni- and bilateral thermal shocks. In the bilateral CTS the temperature is abruptly (in about 10 seconds) raised from 50 °C up to 200 °C, held at 200 °C in order to allow overall heating of the

specimen, and then dropped down to 50 °C. In the unilateral CTS the oil temperature is slowly raised from 50 °C to 250 °C in order to avoid thermal stresses and afterwards fast dropped down to 50 °C.

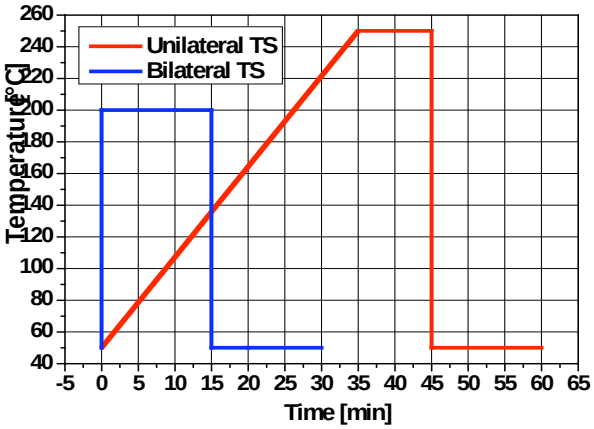

Fig. 4: Uni- and bilateral thermal shocks: Triangular profile Λ 250 °C - 50 °C and rectangular Π 50 °C – 200 °C - 50 °C. The transition time for the temperature shock is about 10 seconds.

3.4 Observed Cracks

It was the goal of the thermo-shock experiments to initiate cracks and to provoke crack growth. For detecting the induced cracks and their length, the experiments had to be interrupted periodically after a certain number of cycles in order to allow the inspection of the samples by scanning electron microscopy (SEM). Fig. 5 shows the initial notch geometry, whereas Fig. 6 illustrates the crack advance for a certain specimen after applying 267, 517, 1287 and 2005 bilateral CTS. After inspecting the specimens, they were mounted again for applying further load cycles. It is worth mentioning that the inspection is limited to the specimen's surface. This limitation is a disadvantage because the stress state in the bulk is expected to be plane strain, whereas at the surface it is plane stress, meaning that first crack initiation is expected to appear in the bulk before they are visible on the surface.

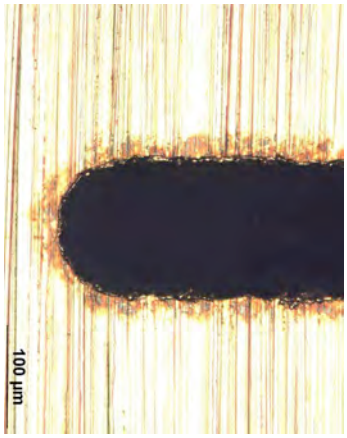

Fig: 5: Initial condition of 1 x 0.1 mm notch before thermal cycling (observed by light microscopy)

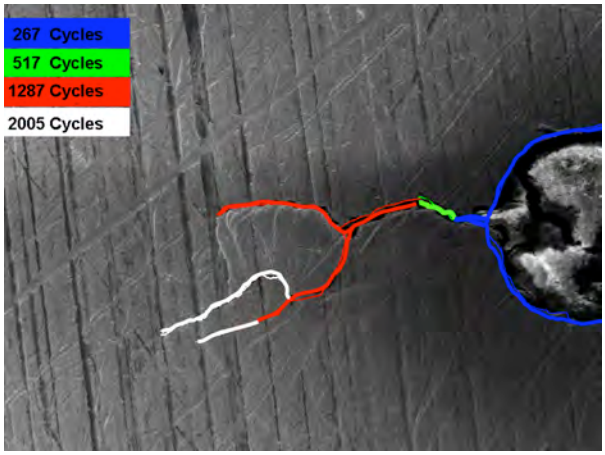

Fig. 6: Crack advancement in austenitic stainless steel due to cyclic bilateral thermal shocks, observed by periodical SEM analyses.

Due to the time consuming CTS experiments only results up to 2000 cycles are available yet. The measured crack growth for the three tested materials and the two different notches are shown in the figures 7 to 9. Each curve represents the averaged results of five equal specimens for each material and load profile. Whereas AISI 347 and AISI 321 showed almost the same crack lengths, shorter cracks appeared in AISI 316L as far as observed in the ongoing experiments. It also turned out that the cracks for the bilateral load are longer than for the unilateral one. However, it has to be kept in mind that the temperature difference for the bilateral CTS was +/- 50 °C, whereas in the unilateral CTS it was -200 °C. Furthermore, the cracks for the 1 mm deep notch grew somewhat faster than for the 0.5 mm notch.

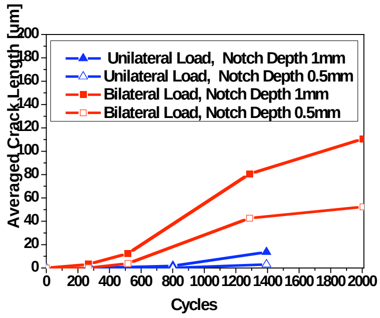

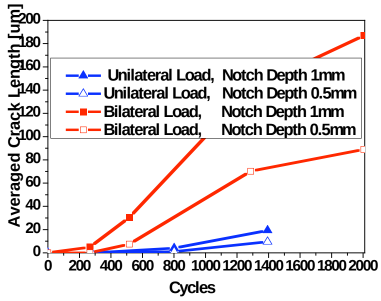

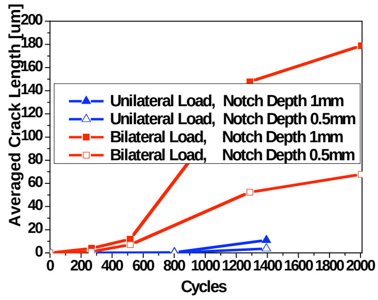

Fig. 7: Crack growth in AISI 316L **Fig. 8:** Crack growth in AISI 321 **Fig. 9:** Crack growth in AISI 347

4 LOW CYCLE FATIGUE TESTS ON STANDARD FATIGUE SPECIMENS

Extensive testing and characterization of the material grades used in the CTS experiments was performed in order to gain the properties for the precise mechanical calculations. Mainly strain controlled isothermal low-cycle fatigue testing (according to ASTM 606-4) on standard fatigue specimens was performed on a servo-hydraulic testing machine in the material testing laboratory at PSI. Fatigue testing with sinusoidal strain amplitudes $\Delta\varepsilon/2$ of +/- 0.2% up to +/-1% yields the number of cycles to crack initiation as well as the cyclic stress-strain curves in the range of RT up to 243 °C. Furthermore, the evolution of stress-strain, i.e. the cyclic hardening and softening, is observed. These data are used to develop advanced material models for the exact numerical prediction of crack initiation due to CTS.

In the experiments performed at room temperature (RT), the increase of the specimen temperature due to plastic deformation is measured and the frequency of the loading cycles is chosen such that the temperature of the specimen is less than 40˚C (0.5 Hz for $\Delta\varepsilon_{tot}/2 < 0.004$ and 0.1 Hz for $0.004 < \Delta\varepsilon_{tot}/2 < 0.01$). For the tests at higher temperatures the required temperature of the specimen was controlled by the furnace.

The numbers of cycles to crack initiation (load drop of 5 %) obtained for a certain strain amplitude and steel grade are shown in Fig. 10. It is worth mentioning that Fig. 10 includes the results for all temperatures within the investigated range. Neither the steel grade nor the temperature had a relevant effect on the fatigue life in spite of the different cyclic hardening/softening behaviour. As shown in Fig. 10, within the investigated strain range the test results are in good agreement with the ASME III mean and the new ANL curve.

The three grades of austenitic stainless steel differ in their hardening/softening behaviour. Figs. 11-16 show the evolution of the maximal and minimal stresses within the loops at RT and 243 °C. At RT AISI 321 shows hardening, softening and secondary hardening, whereas AISI 316L shows only hardening. AISI 347 shows hardening, softening and secondary hardening. The specimens with high yield strength (AISI 321 and 347) showed softening and relevant hardening (probably due to martensite formation) at RT. In the specimens with a normal yield strength level for the solution annealed austenitic stainless steel showed initial hardening followed by a stationary phase. At 243 °C, all materials showed softening with or without subsequent stabilization. At T=243°C only AISI 321 shows initial hardening followed by softening, whereas AISI 316L only shows softening. AISI 347 shows softening already from the first cycle on.

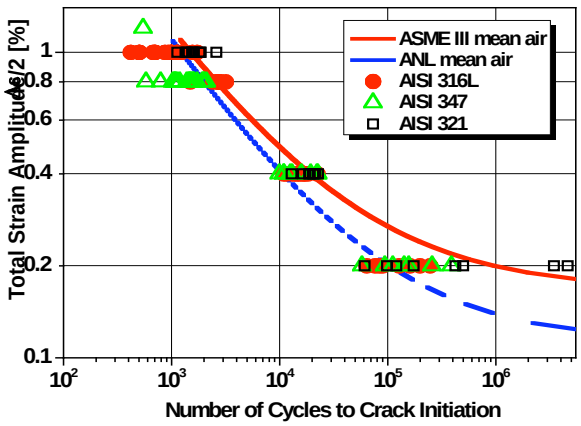

Fig. 10: Number of cycles to failure vs. total strain amplitude for AISI 316L, AISI 347 and AISI 321 in the temperature range from 20 °C to 245 °C.

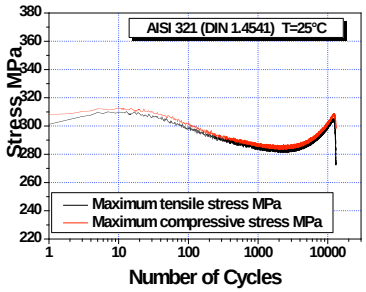

Fig. 11: Max. and min. stress evolution showing hardening, softening and secondary hardening AISI 321, Δε/2 = 0.4 %.

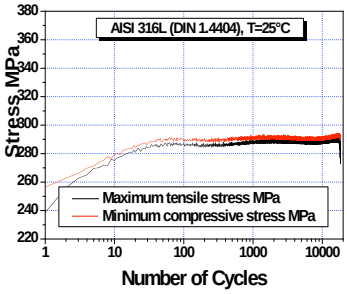

Fig. 12: Max. and min. stress evolution showing hardening of AISI 316L, Δε/2 = 0.4 %.

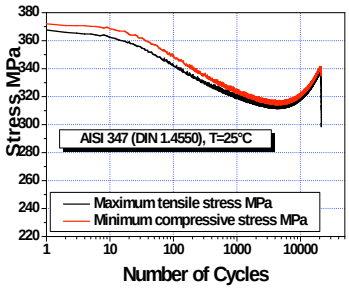

Fig. 13: Max. and min. stress evolution showing hardening, softening and secondary hardening of AISI 347, Δε/2 = 0.4 %.

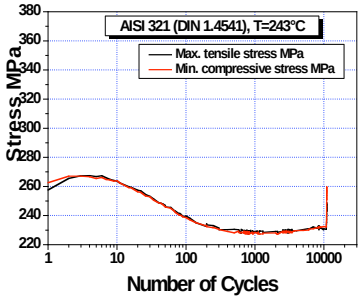

Fig. 14: Maximal and minimal stress evolution showing hardening, softening AISI 321, Δε/2 = 0.4 %.

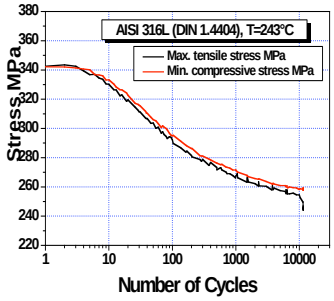

Fig. 15: Maximal and minimal stress evolution showing softening of AISI 316L, Δε/2 = 0.4 %.

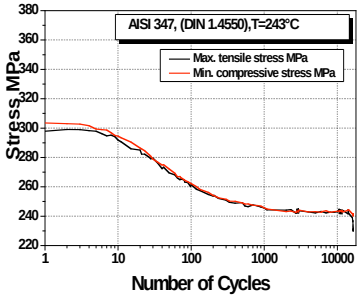

Fig. 16: Maximal and minimal stress evolution showing softening of AISI 347, Δε/2 = 0.4 %.

5 NUMERICAL EVALUATION OF THE CYCLES TO CACK INITIATION IN NOTCHED TEST SPECIMENS DUE TO CYCLIC THERMAL SHOCKS

5.1 Iterative Determination of Heat Transfer using Measured Temperature Profiles

For the calculation of the thermal stresses it is essential that the temperatures calculated in the antecedent step precisely agree with those in the experiment. Since the thermal parameters needed for the calculation are not precisely known, they were iteratively adjusted until agreement between measured and calculated temperatures was reached. These parameters are the specific heat, the heat conductivity of the specimen, the heat-transfer coefficient between oil and specimen and the convection coefficient between specimen and air

(40 W/m^2). All these parameters are considered to be temperature dependent. The heat-transfer coefficient used in the calculation was evaluated for both types of CTS as a function of the temperature difference between oil and the inner wall of the specimen.

For measuring the temperature evolution a specimen was prepared with thermocouples (TC) at several locations within the sample. The radial distance of the TC measured from the inner wall are TC 1=0.5 mm, TC 2=1.0 mm, TC 3=2.0 mm, TC 4=4 mm, TC 5=8 mm and TC 6=16 mm. The measured temperatures are compared with calculated ones in order to adjust heat capacity, heat conduction and heat-transfer coefficients between the oil and the inner wall used in the numerical calculation.

In Fig. 17 and 18 the measured and calculated transient temperature profiles for the bilateral and the unilateral CTS are compared using the heat-transfer coefficients found by the above mentioned iterative procedure. A very good agreement between measured and calculated temperatures was achieved which is the basis for accurate stress/strain calculations.

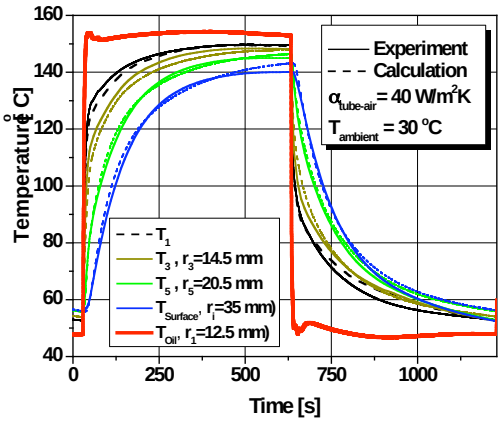

Fig. 17: Comparison of measured and calculated temperature profiles for the bilateral thermo-shock after the iterative evaluation of heat-transfer coefficients.

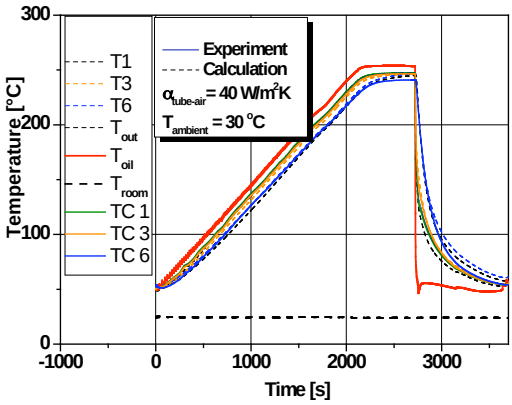

Fig. 18: Comparison of measured and calculated temperature profiles for the unilateral thermo-shock after the iterative evaluation of heat-transfer coefficients.

5.2 Stress/Strain Calculation

In a decoupled, 2D plane strain thermal stress analysis, the specimens are submitted to a cyclic thermal load. The transient stress calculation is based on the antecedent temperature calculation. The main problem of building the mesh of the notched sample is the large difference in size that has to be bridged. Near the notch the mesh has to be very fine in order to capture the local character of the stress gradients at the notch. Such fine meshes have to be handled carefully because of numerical problems which may occur during the calculation (strain localization if softening is considered), further difficulties may appear in the post processing due to the precision of the internal number representation which is in the order of element size).

The cyclic-plastic properties are derived by fitting the experimental data, available from the uniaxial fatigue tests, to the cyclic stress-strain data obtained from simulated cyclic deformation using a nonlinear, cyclic hardening model. The model applied in the finite element simulation is a nonlinear, mixed isotropic-kinematic model with a von Mises yield surface, defined by the function

$$F = f(\bar{\sigma} - \bar{\alpha}) - \sigma_y = 0 \qquad (1)$$

with $\bar{\sigma}$ the stress tensor, $\bar{\alpha}$ the back stress tensor, σ_y the yield stress and f the equivalent von Mises stress potential [Simulia Abaqus Analysis User's manual (2007)]. Observe that the model does not use the conventional 0.2 % strain as a yield limit, but takes into account smaller-strain plasticity, thereby allowing a correct representation of the plastic hysteresis observed in the fatigue experiments.

Omitting temperature and rate dependencies, the kinematic component of the hardening law implemented is

$$\dot{\bar{\alpha}} = \frac{C}{\sigma_y}(\bar{\sigma} - \bar{\alpha})\dot{\varepsilon}_{\text{epl}} - \gamma\bar{\alpha}\dot{\varepsilon}_{\text{epl}} \tag{2}$$

with $\dot{\varepsilon}_{\text{epl}}$ the equivalent plastic strain rate. C and γ are material parameters calibrated to experimental data available from standard fatigue tests [Simulia (2007)]. The dependence of the hardening law on temperature and strain rate is not taken into account. One should also note that the cyclic hardening model does not account for differences in hardening that may be caused by differences in loading strain or strain path.

The number of cycles needed for crack initiation was evaluated based on the local cyclic strain amplitude and the fatigue life curve which was corrected due to Smith-Watson-Topper (SWT) in order to take into account of the non-vanishing mean stresses and the special notch geometry [Smith (1970)]. These factors were found in dedicated additional fatigue tests on notched specimens [Janssens (2009)]. The calculated number of cycles to crack initiation listed in Tab. 1 are somewhat below the experimentally observed ones.

Fig. 19 shows the strain paths observed in the simulations for a rectangular (bilateral) and a triangular (unilateral) temperature loading profile. For the rectangular temperature loading, *compressive* ratcheting is observed, while for the triangular loading, *tensile* ratcheting is calculated. One can also observe that the compressive ratcheting disappears after about 700 cycles, while the tensile ratcheting seems to persist for the number of cycles computed. For the interpretation of these results it is important to consider that ratcheting is limited to a very small area at the root of the notch.

Table 1: Computational and experimental estimate of the number of cycles to crack initiation.

Temperature Loading Profile (°C)	Steel Grade (AISI)	Notch Radius (mm)	Maximum Stress (MPa)	Strain Amplitude (-)	Calculated Number of Cycles to Crack Initiation	Experimentally Observed Number of Cycles to (Micro)Crack Initiation
■ 50-200-50	316L	0.05	345	0.0316	254	500
▲250-50	316L	0.05	365	0.0175	574	800

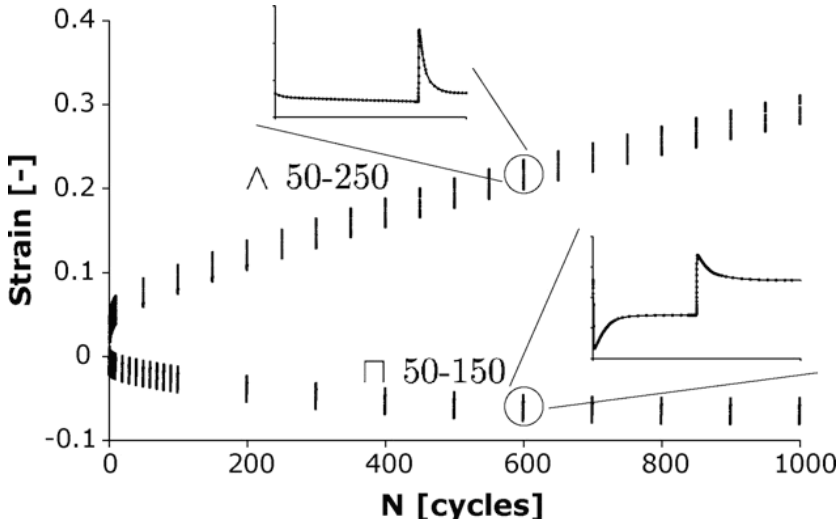

Fig. 19: Strain evolution observed at the notch for a rectangular temperature loading profile (Π 50-150-50) and for a triangular (unilateral) one Λ 250-50). Rectangular (bilateral) loading leads to compressive ratcheting, triangular loading to tensile ratcheting. Note that not all cycles are plotted for reasons of clarity.

Unfortunately, very little experimental information regarding the influence of ratcheting on the number of cycles to fatigue crack initiation is available in literature. The publications known to the authors of this report only address the plastic behaviour of the material, concern highly compressive hydrostatic stress states as in railway applications, or address a ratcheting ratio which is much larger than the ratio of interest to the current experiments.

6 CONCLUSION, DISCUSSION AND OUTLOOK

The ongoing research activities at PSI in the field of thermo-mechanical fatigue are discussed. In particular, a cyclic thermal shock facility allowing experiments under well defined loading and boundary conditions is described. The experiments were successful in that short cracks were initiated in notched ring-shaped test specimens for both load types in the steel grades AISI 347, AISI 316L and AISI 321, by pure thermal load-

ing. These cracks appeared often with a bifurcated shape and in several cases two or more cracks has been developed. However, as a consequence of the low frequency of the shock cycles result up to only 2000 cycles are available yet for the presented specimens and all crack lengths are still below 0.5 mm. Even the experimental results have to be consolidated in the continuation of the project, they already allow to compare the three materials concerning their susceptibility for crack initiation. The question whether cracks grow through the wall under the applied cyclic thermal loading conditions, as predicted by the calculations (not described in this presentation), thus remains unanswered. Different crack lengths were identified for unilateral and bilateral thermal shocks.

Extensive material testing and characterization provided the material properties needed for the precise mechanical calculations. Based on the measured cyclic elasto-plastic stress-strain curves, which include both hardening and softening, FE models were built to capture this complex behaviour. The calculated number of cycles needed to initiate cracks agrees within an acceptable tolerance with those evaluated in the experiments. The calculation of number of cycles to crack initiation is based on the lifetime curves evaluated in uniaxial fatigue testing. It was found that Smith-Watson-Topper (SWT) correction can be successfully applied to predict the number of cycles to crack formation, if notch-specific calibration factors are used in the SWT correction.

We conclude that valuable experimental and numerical results have been obtained in the first project period. These results need to be consolidated in the ongoing project phase (2010-2011). The continuation of the project will be focussed on the calculation of crack growth by the Extended Finite Element method, the improved CFD simulation and special aspects of cyclic plasticity.

Acknowledgements. *We are grateful to swissnuclear for the financial support of the PLiM project. Our thank is also addressed to our project partner Siempelkamp Prüf- und Gutachtergesellschaft GmbH in Dresden for performing the thermal shock experiments. Special thank goes to Mr. P. Simon for the analysis of the thermal shock specimens and to our colleagues Dr. Brian Smith, Dr. S. Kuhn and Dr. B. Niceno for contributing the CDF modeling.*

REFERENCES

Cipiere, M.F., Le Duff, J.A., July 1, 2001. Thermal fatigue experience in French piping, influence of surface condition and weld local geometry, Document IIW-XII-1891, Ljubljana, Slovenia.

Cipiere, M.F., Goltrant, O., September, 2002. Circuit RRA N4, Incident de Civaux 1, Fontevraud 5, Volume 2, pages 875-882, 23-27.

Deardorff, A. et. al., October 2004. A Survey of Current US Nuclear Plant Fatigue Issues, International Conference on Fatigue of Reactor Components, Seville, Spain, 4-6.

Faidy, C., July 31- August 2, 2000Thermal fatigue in French RHR systems, International conference on fatigue of reactor components, Napa.

Hirshberg, P., July 31-August 2, 2000. Opearting experience regarding thermal fatigue of un-isolable piping connected to PWR reactor coolant systems, International Conference on Fatigue of Reactor Components, Napa.

Janssens, K.G.F., Niffenegger, M., Reichlin, K., 2009. A computational fatigue analysis of cyclic thermal shock in notched specimens, Nuclear Engineering and Design Vol. 239. P. 36–44.

Lässig, S., 2007. Thermomechanische Ermüdung infolge zyklischem Thermoschock, Diplomarbeit, Hochschule Mittweida (FH).

NEA, Thermal cycling an LWR components in OECD-NEA member countries, CSNI integrity and ageing-working group, NEA/CSNI/R(2005)8.

Simulia (Abaqus Analysis User's manual), 2007 volume 3, page 18.2.2. Dassault Systemes Simulia. http://www.simulia.com/.

Smith, K. N. and Watson, P. and Topper, T. H., 1970, A stress-strain function for the fatigue of metals J. Mater. Vol. 5 No. 4 pp. 767-778.